

FINAL REPORT

Current Flow in the Magnetosphere  
during Periods of Moderate Activity  
by

Gordon Rostoker & T.J. Hughes

EPB  
Open File  
77-21

This document was produced  
by scanning the original publication.

Ce document est le produit d'une  
numérisation par balayage  
de la publication originale.



Energy, Mines and  
Resources Canada

Énergie, Mines et  
Ressources Canada

Earth Physics Branch Direction de la physique du globe

---

1 Observatory Crescent  
Ottawa Canada  
K1A 0Y3

1 Place de l'Observatoire  
Ottawa Canada  
K1A 0Y3

GEOMAGNETIC SERVICE OF CANADA

Current Flow in the Magnetosphere During Periods  
of Moderate Activity

Gordon Rostoker and T.J. Hughes

35 pp.  
Price \$7.00

Earth Physics Branch Open File No. 77-21  
Ottawa, Canada  
1977

NOT FOR REPRODUCTION

FINAL REPORT

CURRENT FLOW IN THE MAGNETOSPHERE  
DURING PERIODS OF MODERATE ACTIVITY

BY

GORDON ROSTOKER AND T.J. HUGHES

EMR CONTRACT OSQ5-0019.

DSS FILE NUMBER SQ15.23235-5-0045

MARCH 31, 1976

Earth Physics Branch Open File 77-21

FINAL REPORT

Current Flow in the Magnetosphere During Periods of  
Moderate Activity

---

EMR Contract OSQ5-0019

DSS File Number SQ15.23235-5-0045

Principle Investigator (Contractor)

Dr. Gordon Rostoker  
Associate Professor of Physics  
University of Alberta

Coinvestigators

Mr. T.J. Hughes  
Dr. R.P. Sharma

Abstract The object of this research was to upgrade existing knowledge of high latitude current systems in order to facilitate co-ordinated research during the upcoming International Magnetospheric Study (1976-1979). Emphasis was laid on the recently discovered phenomenon of net field-aligned current flow into and out of the auroral oval. It was found that net downward current flow exists across the region of the westward electrojet over a large range of local times in the dawn sector. The net upward current flow is confined to the pre-midnight quadrant, and tends to be concentrated near the poleward border of the eastward electrojet. In the Harang discontinuity between the eastward and westward electrojet, the current flow involves a strong poleward Hall current and a westward Pedersen current. The current flow pattern is related closely to the auroral zone electric field configuration obtained by Mozer and Lucht (1974). Net field-aligned current flow is found to contribute significantly to the overall magnetic perturbation pattern at high latitudes, and is thought to be the source of the Hall current electrojets.

## Introduction

Over the last few years, the understanding of current flow at high latitudes has increased significantly. In retrospect, one may look at the work of Harang (1946) as the study which first showed the electrojet structure in what is now known as the auroral oval. This electrojet configuration is shown in Figure 1a, after a modification by Sugiura and Heppner (1965). Such a configuration would imply that the auroral oval is a single entity, with current flow being continuous through the high conductivity zone. However, it is now becoming recognized that there is a significant difference between the dayside auroral oval (which maps to the polar cleft) and the nightside oval (which maps to the plasma sheet). Langel (1974) has shown that there is a significant difference between eastward jet flow in the post-noon quadrant and the eastward electrojet in the pre-midnight quadrant, and has proposed the high latitude equivalent current system shown in Figure 1b. Based on several years of study of the University of Alberta magnetometer line data, we feel that Figure 1b is the best equivalent current system yet proposed for high latitude regions.

It is, of course, important to recognize that the patterns shown in Figure 1 are equivalent current systems,

and are simply an effective means of portraying the magnetic perturbation pattern observed at the surface of the earth. The real current flow most certainly involves field-aligned currents, which are sure to flow wherever there are conductivity discontinuities. First proposed by Birkeland (1908, 1913) and reintroduced by Kern (1962) and Boström (1964), field aligned currents were accepted as a component of the high latitude current flow some time before their identification by in situ measurements using magnetometers in polar orbiting satellites (Zmuda et al., 1967). Subsequent studies of the gross Birkeland current flow by Armstrong and Zmuda (1970), and Zmuda and Armstrong (1974) led to a consistent picture of the relationship of high latitude ionospheric parameters to field-aligned current flow shown in Figure 2.

While Zmuda and Armstrong (1974) felt that, on the average, the field-aligned current flow integrated along a meridian was zero (Viz., there was as much upflowing current as downflowing current) it has become clear that this is generally not the case. In particular, Yasuhara et al. (1975) and several studies by Potemra and colleagues (Sugiura and Potemra, 1975; Iijima and Potemra, 1975) show that there is a tendency for there to be net downward current flow in the morning sector and net upward flow in the evening sector. If this is indeed the case one would expect to see distinctive magnetic signatures at ground based observatories,

which will have the basic characteristic of a level change in the east-west (D) component. The study described in this report yields the diurnal variation of the disturbance component of the magnetic field associated with the net field aligned current flow and presents a description of the real current flow in the ionosphere and magnetosphere.

#### Description of Data Suite and Analysis Technique

The primary suite of data utilized in this study is from the University of Alberta magnetometer line during a period of operation from Day 332, 1971 to Day 24, 1972. Each station on the line is equipped with a three-component fluxgate magnetometer and digital recording system. Measurements by the system are accurate to  $\pm 1$  nT over a range of  $\pm 1000$  nT, and timing is considered accurate to  $\pm 0.1$  sec. (except at Contwoyto Lake where timing difficulties reduced the accuracy to  $\pm 20$  sec.). The coordinates of the eight digital observatories used in this study are listed in Table 1. In addition, two observatories (Resolute Bay ( $83.0^{\circ}$ N) and Newport ( $55.1^{\circ}$ N)) are operated on the  $300^{\circ}$ E meridian by other agencies and their data were utilized on our study to supplement the meridian line data.

For use in this study, the data were manipulated to produce hourly averaged values (centered on the half hour)

Table 1

## Coordinates and L Values of Magnetometer Line Sites

Site	Code Name	Geographic		Geomagnetic		L R <sub>E</sub>
		Latitude (°N)	Longitude (°E)	Latitude (°N)	Longitude (°E)	
Cambridge Bay	CAMB	69.1	255.0	76.8	296.6	19.5
Contwoyto Lake	CONT	65.5	249.7	72.6	295.8	11.3
Fort Reliance	RELI	62.7	<i>109.8</i> 251.0	70.3	300.1	8.9
Fort Smith	SMIT	60.0	<i>111.5</i> 248.0	67.3	300.0	6.8
Fort Chipewyan	FTCH	58.8	<i>112.09</i> 248.0	66.3	303.1	6.2
Fort McMurray	MCMU	56.7	<i>111.27</i> 248.8	64.2	303.5	5.4
Meanook	MENK	54.6	246.7	61.9	300.8	4.5
Leduc	LEDU	53.3	<i>113.3</i> 246.5	60.6	302.9	4.2



of each component at each station and latitude profiles were constructed for each hourly interval of each day. The horizontal components (H, D) were rotated so that the perturbation components of the field are presented in the geomagnetic (centered dipole) system. Based on the perturbation pattern from the net field aligned current flow expected at the surface of the earth, the latitude profiles were then interpreted in terms of the diurnal characteristics of that current flow.

#### Interpretation Techniques

Using latitude profiles of the type shown in Figure 3 we are able to infer information about the latitudinal and longitudinal extent of the magnetospheric-ionospheric current flow, along with positions of the poleward and equatorward borders of the electrojets and the current intensity (see Rostoker, 1972; Kisabeth, 1972). More recently, inversion techniques (Oldenburg, 1976) permit us to evaluate the distribution of current across the latitudinal extent of the electrojet. In Figure 3a we see the model latitude profile for a three dimensional current loop whose ionospheric segment is a westward electrojet with a width of  $5^{\circ}$  and a length of  $20^{\circ}$  centered at a geomagnetic latitude of  $67.5^{\circ}\text{N}$ . A model profile is also shown in Figure 3b for the case of an identical three dimensional current, except that the current density has a gaussian distribution across the electrojet.

The negative H-regime under the center of the electrojet is due to the ionospheric electrojet whose contribution is decreased by the effects of the field aligned currents at the ends of the electrojet and increased somewhat by earth induction effects. The Z-component is reduced somewhat by earth induction effects, but the peaks in  $\Delta Z$  essentially mark the latitudinal borders of the electrojet region. The D-component is primarily due to the field aligned currents - for a very long electrojet  $\Delta D$  would be zero over the entire latitude profile sufficiently far from the ends of the electrojet. For the steady state auroral electrojet the assumption of a long electrojet away from the noon and midnight regions is valid. In Figure 3c we show an hourly averaged latitude profile from the meridian line of stations where  $\Delta D$  does not exhibit a polarity transition across the center of the electrojet (as might be expected looking at Figure 3a). However  $\Delta D$  is biased positive across the electrojet region due to the equatorward flow of Hall current associated with the eastward electric field known to exist in this local time sector (Rostoker et al., 1974; Mozer and Lucht, 1974). Any level change due to net field aligned current flow will be superposed on this positive bias in  $\Delta D$ .

Finally, we point out that, particularly in the dusk sector, the station line often cuts the electrojet at an angle which deviates significantly from  $90^\circ$ . For such cases, the perturbation due to the ionospheric electrojet appears in

both the H and D components. This effect is easily identified because the D-component tends to track the H-component across the latitudinal extent of the electrojet as shown in Figure 4a. In order to properly interpret the latitude profile it was necessary to transform the data into a co-ordinate system such that the electrojet was normal to the newly defined north-south component direction for the data. This was done in the following fashion. It was assumed that the current distribution across the electrojet was parabolic in form. The components H and Z were then fitted to the current system using linear regression techniques to establish the width and total current of the system. Then H, D and Z were used to yield the angle of tilt of the electrojet to the station line; this was done by subtracting the observed  $\Delta D$  from the modelled  $\Delta D$ , and fitting a Heaviside step function to the residual (which then represents the level change due to the net field aligned current flow.) The result of this procedure on the data shown in Figure 4a is presented in Figure 4b.

Finally, each latitude profile was interpreted to determine whether or not there was any net field aligned current flow and, if so, the direction of that flow. The results of our analysis are shown in the following section.

## Results

The primary result stemming from this study is the separation of the region of disturbance associated with steady state processes in the magnetosphere into five distinct regimes.

Starting from  $\sim 2200$  LMT the region spanning local magnetic midnight (termed the Harang discontinuity) to  $\sim 0200$  LMT forms one distinct region. A typical latitude profile descriptive of this region is shown in Figure 5. (Local magnetic midnight is approximately 0830 UT for our station line near the December solstice). Latitude profiles in this region may show the signature of either the eastward electrojet, the westward electrojet or both jets. (In Figure 5 we see the signatures of both jets.) Of course, it is quite likely that any profile is sensing the end effects of the jets, and signatures such as that shown in Figure 5 do not guarantee either eastward or westward Hall current flow over the station line. The one distinctive feature of the Harang discontinuity is a region of negative  $\Delta D$  across the entire auroral oval region; there is generally a distinctive negative step in  $\Delta D$  across the equatorward border of the auroral oval (as seen in Figure 5). As we shall discuss later in the text, we believe the  $-\Delta D$  signature to be caused by poleward flowing Hall current,

diverging from the eastward and westward Hall current electrojets.

A second distinctive region spans the dawn meridian stretching from  $\sim 0200$  LMT to  $\sim 1000$  LMT. This region is dominated by the westward electrojet, although there are generally traces of eastward current flow just equatorward of the westward electrojet (Rostoker and Hron, 1976). In this region  $\Delta D$  is biased positive across most of the auroral oval due to equatorward Hall current flow associated with an eastward electric field (Rostoker et al., 1974; Mozer and Lucht, 1974). In Figures 6a, 6b, and 6c we see three latitude profiles typical of the region; Figure 6a is taken close to the boundary between this region and the Harang discontinuity, Figure 6b is taken near local magnetic dawn and Figure 6c is taken close to local magnetic noon. The most outstanding feature of this region is the development of a positive step in  $\Delta D$  (going from south to north across the electrojet) which becomes a dominant feature near local magnetic noon. We associate this step in  $\Delta D$  with downward flowing field aligned current; this is the ground based magnetic signature of the net field aligned current flow detected by polar orbiting satellites (Iijima and Potemra, 1975). We believe that this net downward current flow diverges in the ionosphere to flow as Hall current in the westward electrojet. The physics of the divergence process is described in

Heppner et al., (1971). If this were the case, one would expect a change in the ratio of  $\Delta H$  (contributed by the ionospheric Hall current) to the magnitude of the step in  $\Delta D$  (contributed by the field aligned current feed) as a function of local time. The predicted trend would be  $(\Delta D/\Delta H)$  becoming larger as one approaches local magnetic noon, since near local magnetic noon there would be significant downward current flow and little electrojet would have built up while near  $\sim 0300$  LMT, the electrojet will have reached its peak strength while the net field-aligned current flow will have decreased towards zero. For the 42 days treated in this study, we computed  $(\Delta D/\Delta H)$  in the dawn sector from  $\sim 0200$  LMT to  $\sim 1000$  LMT. The average value of this ratio is seen in Figure 7. We see that the ratio slowly increases towards local noon, rising steeply in the two hourly intervals closest to local magnetic noon. Computation of the  $(\Delta D/\Delta H)$  ratio past 1000 LMT was impossible since, although the step in  $\Delta D$  was very distinctive,  $\Delta H$  was completely uninterpretable - that is, it was impossible to identify the westward electrojet. Our data suggest, indeed, that the westward Hall current electrojet is fed by net downward field aligned current flow in this local magnetic time sector.

The third distinctive region spans local magnetic noon from  $\sim 1000$  LMT to  $\sim 1400$  LMT. This region has been identified by Harang (1946) as a zone of confusion, and a cursory

glance at latitude profiles associated with this local time sector makes his evaluation perfectly understandable! Two profiles taken in this local magnetic time region are shown in Figures 8a and 8b. It is probable that  $\Delta H$  and  $\Delta Z$  are influenced by the eastward current flow to the west, the westward current flow to the east and  $sq$  current associated with dynamo effects. While  $\Delta H$  in the two profiles shown are quite different, the distinctive positive step in  $\Delta D$  is clearly apparent in both. In general, we feel that there is no distinctive electrojet pattern in this "zone of confusion", however, there is persistent net downward field aligned current flow.

The fourth distinctive region is the post noon quadrant stretching from  $\sim 1400$  LMT to  $\sim 1900$  LMT (near local magnetic dusk). This region is marked by an absence of net field aligned current flow, although there is clearly a latitudinally confined region of eastward current flow in this sector. A typical latitude profile taken in the sector is shown in Figure 9. The work of Rostoker et al. (1976) has established that the peak in negative  $\Delta Z$  approximately marks the equatorward border of the polar cleft and the poleward border of the eastward electrojet current flow.

The fifth (and final) distinctive region is the evening quadrant, dominated by the  $+\Delta H$  signature of the eastward electrojet. We also find the consistent presence of a negative step in  $\Delta D$  across the poleward portion of the

eastward electrojet, indicative of upward flowing net field aligned current. A typical latitude profile taken in this sector is shown in Figure 10. Magnetic signatures of this nature dominate over the local magnetic time interval of  $\sim 1900 - 2200$ , and the eastward extremity of this regime is adjacent to the Harang discontinuity.

A summary plot describing the regions of upward and downward net field aligned current flow as a function of UT (and LMT) is shown in Figure 11. We find a remarkable similarity between the behavior of the net field aligned current flow as inferred from this diagram and the diurnal variation in the electric field observed in the auroral oval region by Mozer and Lucht seen in Figure 12. Although this plot is for local time variation, it can be related to LMT since most observations were taken in the Western Canadian sector. Then 0000 UT would correspond to 2230-2300 LMT, for the observations by Mozer and Lucht. The correspondence between our data and the electric field data is shown in Table 2.



### Conclusion

From the information we have gained in this study, we are prepared to present a working model of the real current flowing into and out of the auroral oval, along with the ionospheric current in the electrojet regions. This working model is shown in Figure 13. Not shown in this figure are the balanced components of the Birkeland current flow (seen in Figure 2) which cannot be detected by ground based magnetometers unless there are observable end effects. In our model, relatively concentrated downward current flow over the noon sector feeds both the eastward and westward electrojets. The electrical circuits are closed by upward current flow in the pre-midnight quadrant and possibly in the Harang discontinuity. The Hall electrojets have their current flow diverted to the poleward border of the auroral oval in the Harang discontinuity (as evidenced by the westward electric field in that sector), where the current diverges up the field lines into the magnetotail.

In our study we have identified the ground-based magnetic signatures of net field aligned current flow in the magnetosphere, and we have defined distinctive regions of this net field aligned current flow. This information should be extremely useful in using world-wide magnetometer data to describe the state of the magnetosphere during the international magnetospheric study.

TABLE 2

Correspondance Between Net Field Aligned Current Flow and Auroral Zone  
Electric Field

<u>LMT SPAN</u>	<u>REGIME</u>	<u>ELECTRIC FIELD</u>	<u>FIELD ALIGNED CURRENT AND IONOSPHERIC CURRENT FLOW</u>
2200 - 0200	Harang Discontinuity (Midnight Sector	Primarily Westward Poleward toward dusk and Equatorward toward dawn	Poleward Hall current flow Westward Pedersen current flow
0200 - 1000	Dawn Sector	Pronounced eastward com- ponent Consistant Equatorward component	Dominated by westward Hall Current flow; net downward field aligned current regime
1000 - 1400	Noon Sector	Weak eastward component or zero eastward component Confused north-south com- ponent	No pronounced consistent electrojet flow Continued downward net field aligned current flow
1400 - 1900	Post-noon quadrant	Zero east west component	Eastward electrojet flow No net field aligned current flow
1900 -2200	Pre-midnight quadrant	Westward component to- ward midnight edge of regime Consistent poleward com- ponent	Eastward electrojet flow Net upward field-aligned current flow

## References

- Armstrong, J.C. and A.J. Zmuda, Field-aligned current at 1000 km in the auroral region measured by satellite, J. Geophys. Res., 75, 7122, 1970.
- Birkeland, K., The Norwegian Aurora Polaris Expedition, 1902-03 Christiania, Vol. 1, Sect. 1, 1908.
- Birkeland, K., The Norwegian Aurora Polaris Expedition, 1902-03; Christiania, Vol 1, Sect. 2, 1913
- Bostrom, R., A model of the auroral electrojets, J. Geophys. Res., 69, 4983, 1964.
- Harang, L., The mean field of disturbance of polar geomagnetic storms, J. Geophys. Res., 51 353, 1946.
- Heppner, J.P., J.D. Sfolarik, and E.M. Wescott, Electric field measurements and the identification of currents causing magnetic disturbances on the polar cap, J. Geophys. Res., 76, 6028, 1971.
- Iijima, T., and T.A. Potemra, The amplitude distribution of field-aligned currents at northern high latitudes observed by TRIAD, Johns Hopkins/APL Report, August, 1975.
- Kern, J.W., A charge separation mechanism for the production of polar auroras and electrojets, J. Geophys. Res., 67, 2649, 1962.

- Kisabeth, J.L., The dynamical development of the polar electrojets, Ph. D. Thesis, University of Alberta, Edmonton, Alberta, Canada, 1972.
- Langel, R.A., Near earth disturbance in total field at high latitudes 2. Interpretation of data from Ogo 2, 4 and 6, J. Geophys. Res., 79, 2373, 1974.
- Mozer, F.S., and P. Lucht, The average auroral zone electric field, J. Geophys. Res., 79, 1001, 1974.
- Oldenburg, D.W., Ionospheric current structure as determined from ground based magnetometer data, Geophys. J., in press, 1976.
- Rostoker, G., Interpretation of magnetic field variations during substorms, in Earth's Magnetospheric Processes, ed. B.M. McCormac, D. Reidel Publ. Co., 379, 1972.
- Rostoker, G., A.J. Chen, F. Yasuhara, S.-J. Akasofu and K. Kawasaki, High latitude equivalent current systems during extremely quiet times, Planet. Space Sci., 22, 427-437, 1974.
- Rostoker, G., and M.P. Hron, The eastward electrojet in the dawn sector, Planet. Space Sci., 23, 1377, 1975.
- Sugiura, M., and J.P. Heppner, The earth's magnetic field, in Introduction to Space Science, ed. by W.N. Hess, p.45, Gordon and Breach, New York, 1965.
- Sugiura, M., and T.A. Potemra, Net field-aligned currents observed by TRIAD, Johns Hopkins/APL Report, July, 1975.

Yasuhara, F., Y. Kamide and S.-I. Akasofu, Field-aligned and ionospheric currents, Planet. Space Sci., 23, 1355, 1975.

Zmuda, A.J., F.T. Heuring, and J.H. Martin, Dayside magnetic disturbances at 1100 kilometers in the auroral oval, J. Geophys. Res., 72, 1115, 1967.

Zmuda, A.J., and J.C. Armstrong, The diurnal flow of field-aligned currents, J. Geophys. Res., 79, 4611, 1974.

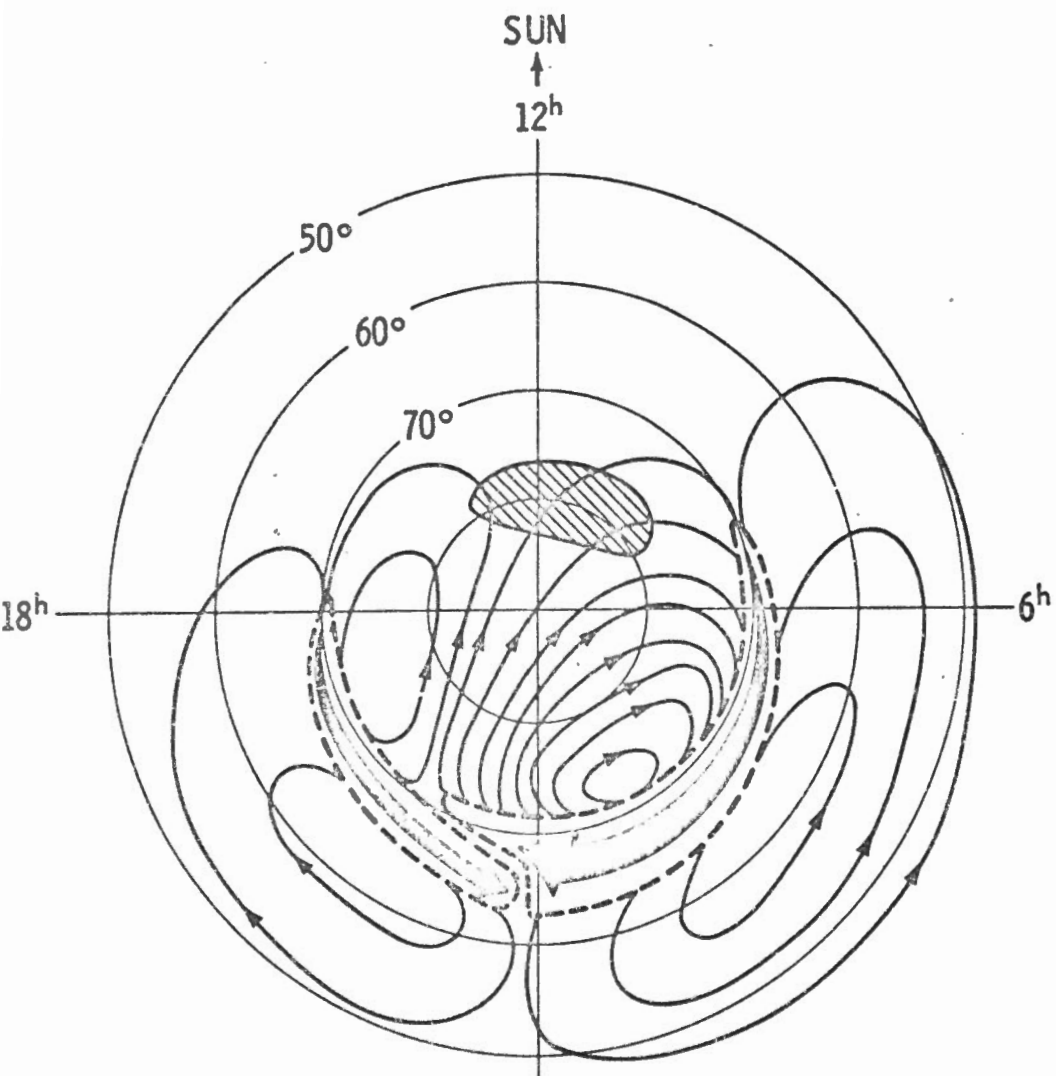


FIGURE 1(a). The East and West Electrojets in the auroral oval. (Sugiura and Heppner (1965)).

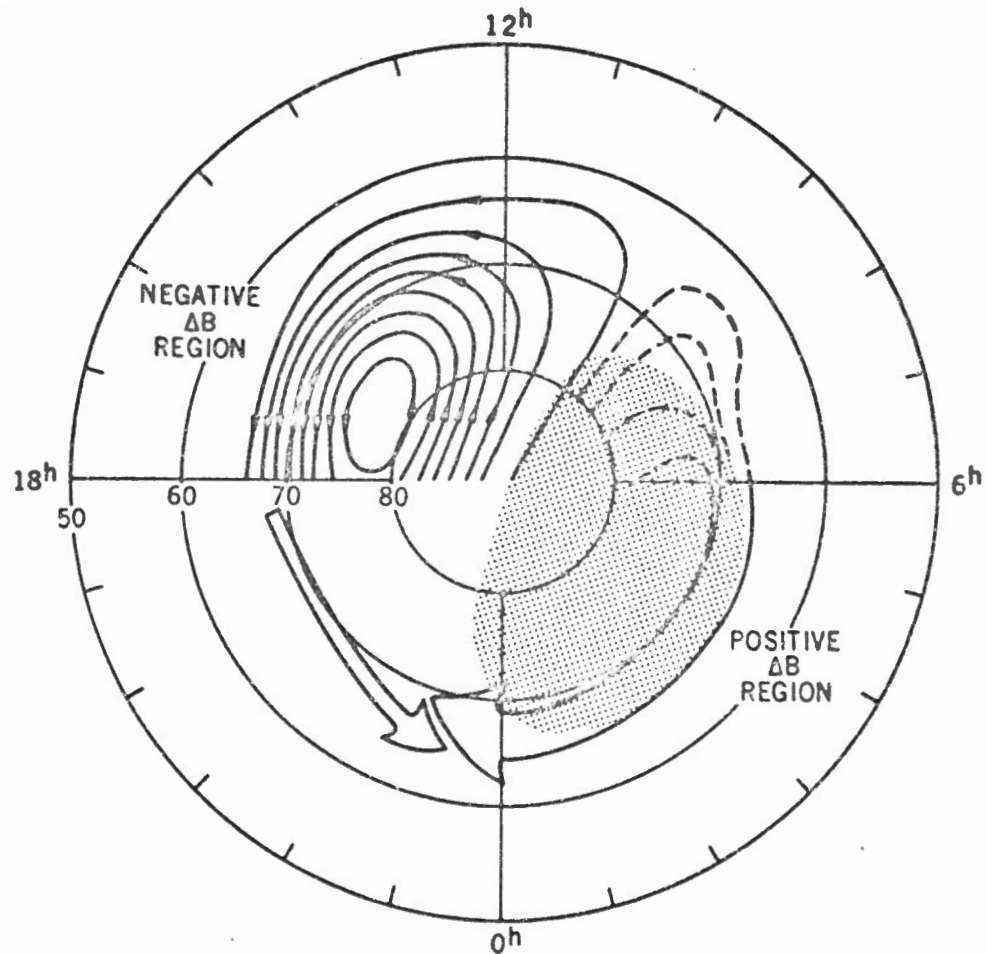


FIGURE 1(b). The high latitude current system proposed by Langel (1974).

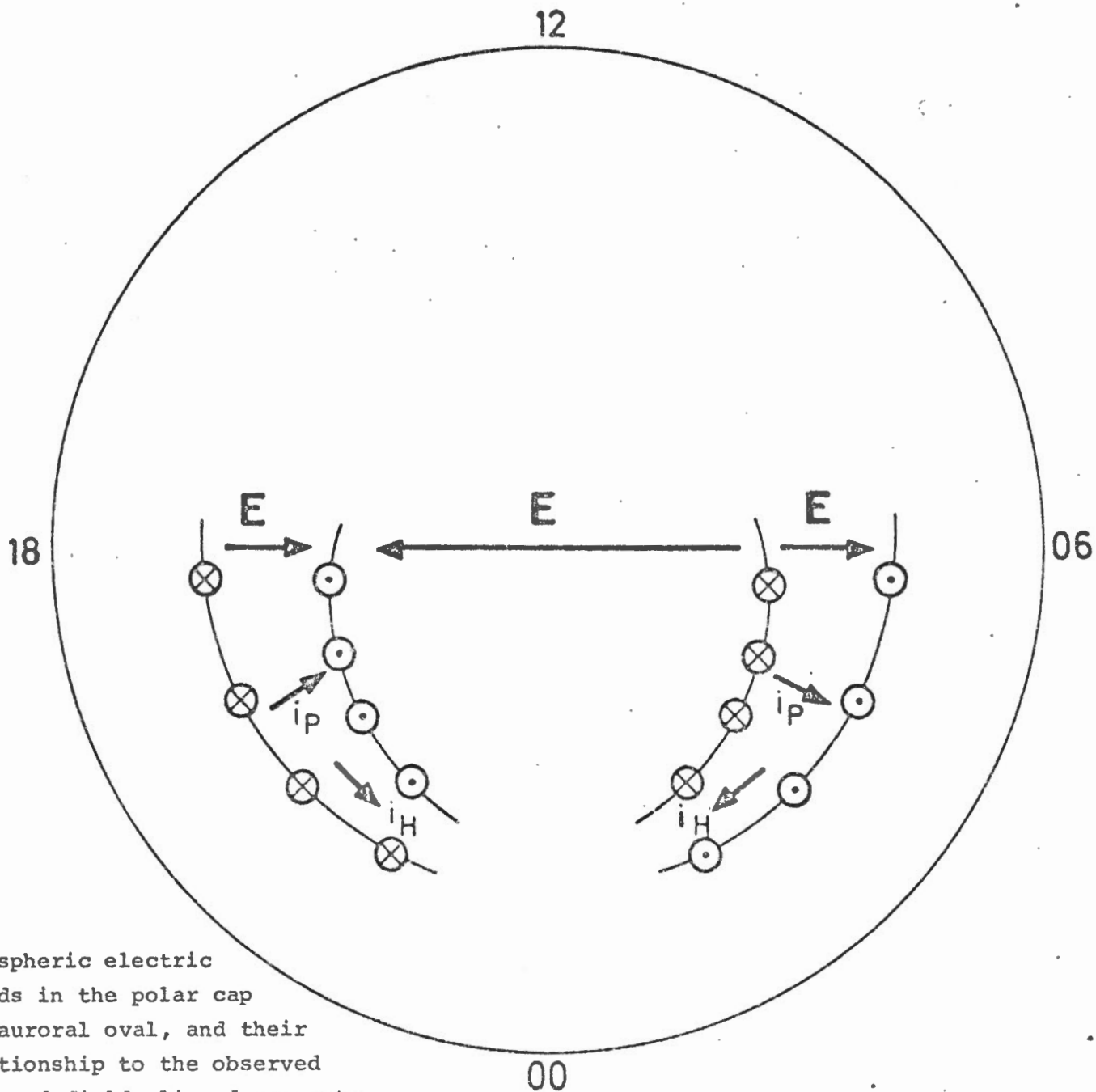
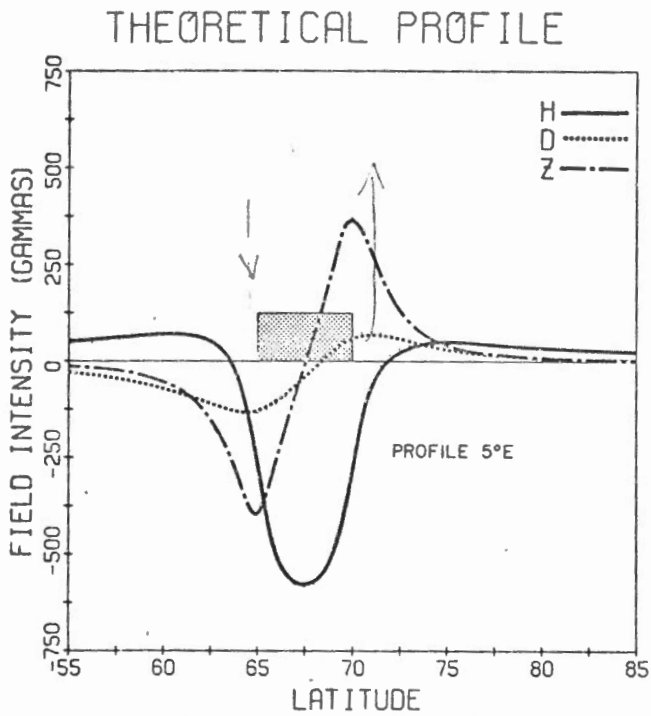
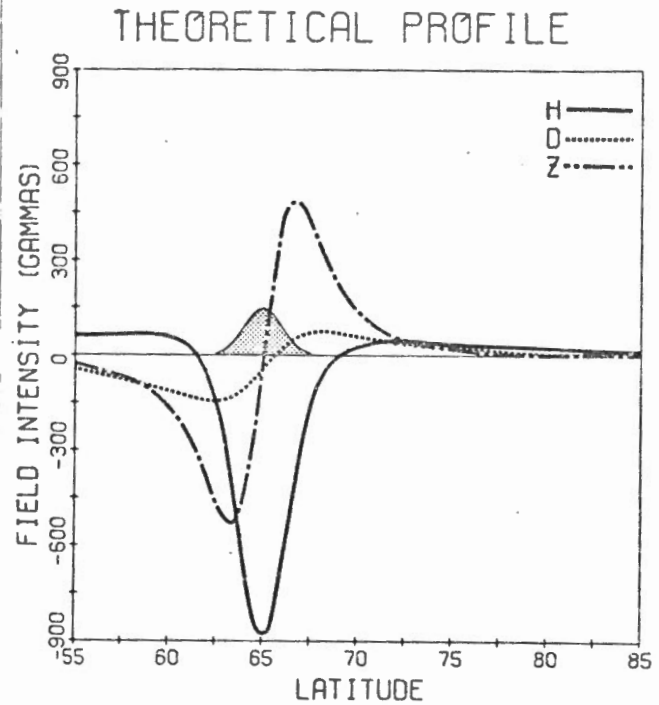


FIGURE 2. Ionospheric electric fields in the polar cap and auroral oval, and their relationship to the observed balanced field aligned currents.



A



B

FIGURE 3(a). Latitude profile of a model three-dimensional current system, with a constant latitudinal current density distribution. The ionospheric portion of the current is confined to 5° of latitude, centred at 67.5°N, and 20° of longitude. The total integrated current is  $1 \times 10^6$  amps. The profile is for a magnetometer chain positioned 5°E of the centre of the current system.

FIGURE 3(b). Latitude profile for a current system similar to that in figure 3(a), except that the current is distributed in latitude according to  $J(x) = \exp(-3x^2)$ , where  $x$  is the distance from the latitudinal centre of the electrojet, which in this case lies at 65°N.



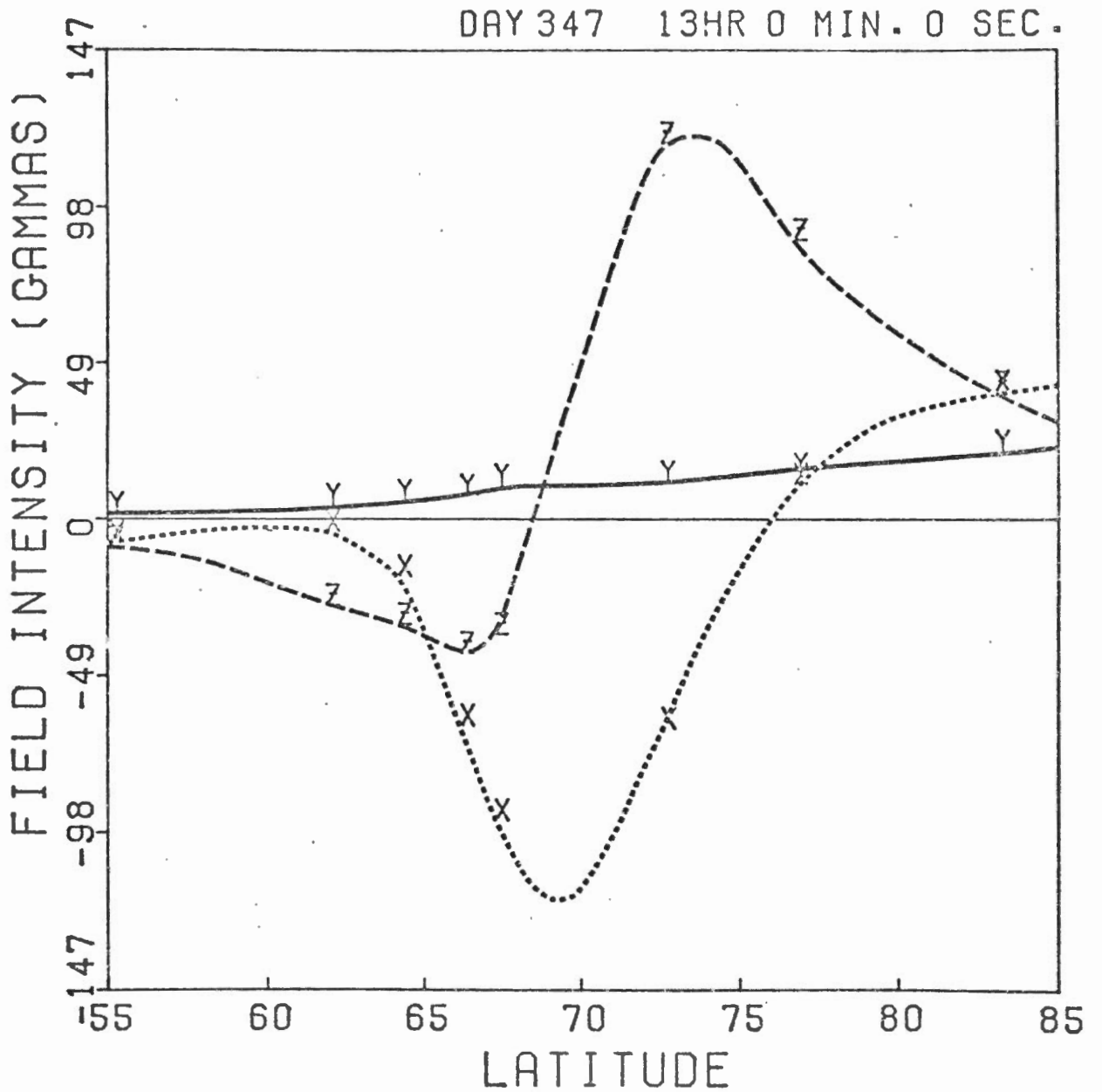


FIGURE 3(c). Hourly average latitude profile for Day 347, Hour 1200-1300 UT. Note the absence of the D(Y) component level shift, and the positive D bias.

DAY 5

3 HR 0 MIN. 0 SEC.

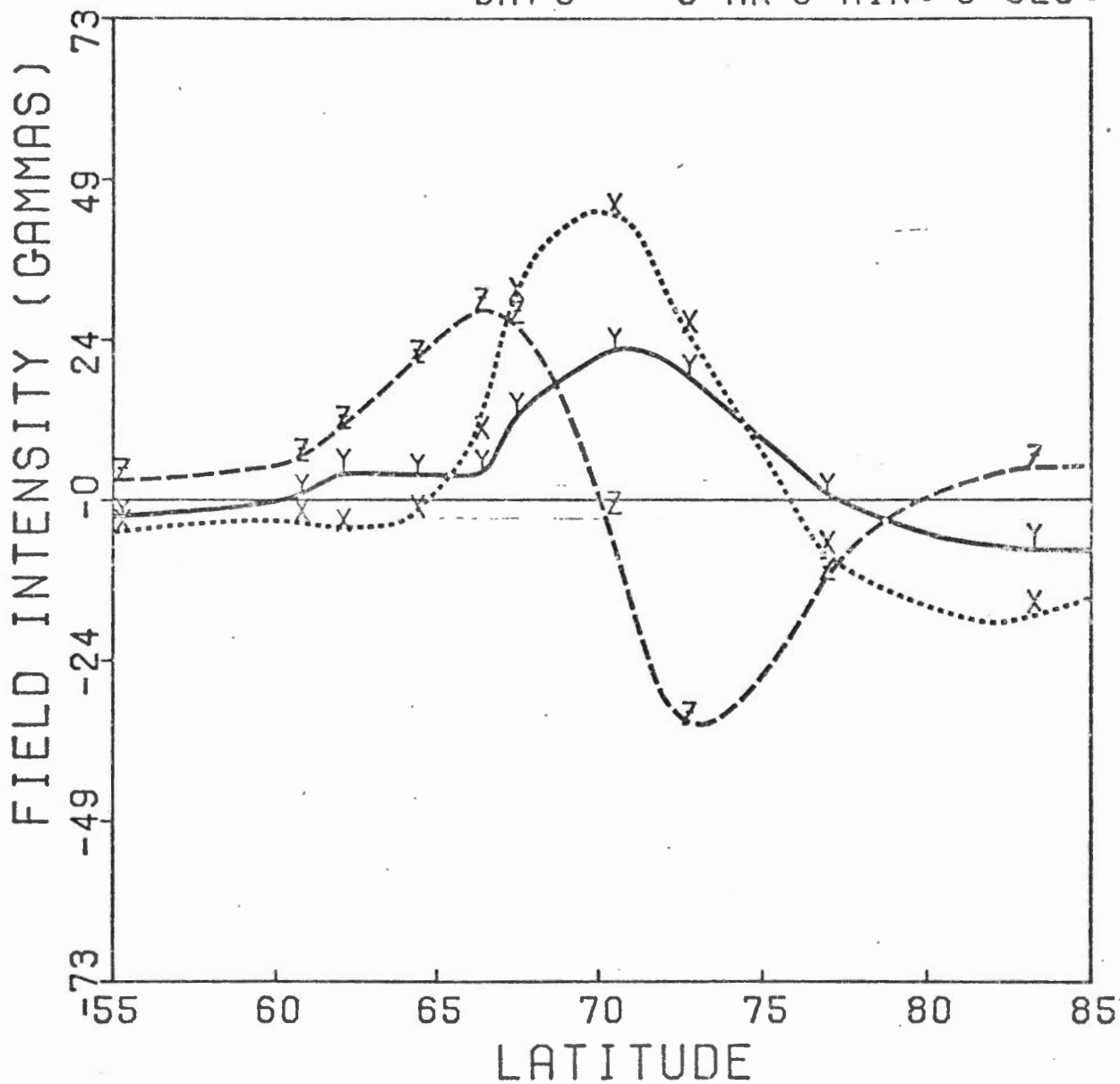


FIGURE 4(a). Hourly average latitude profile for Day 5, Hour 0200-0300 UT. Note the similarity between D(Y) and H(X), indicating that the electrojet was not flowing normal to the station line.

DAY 5 3 HR 0 MIN. 0 SEC.

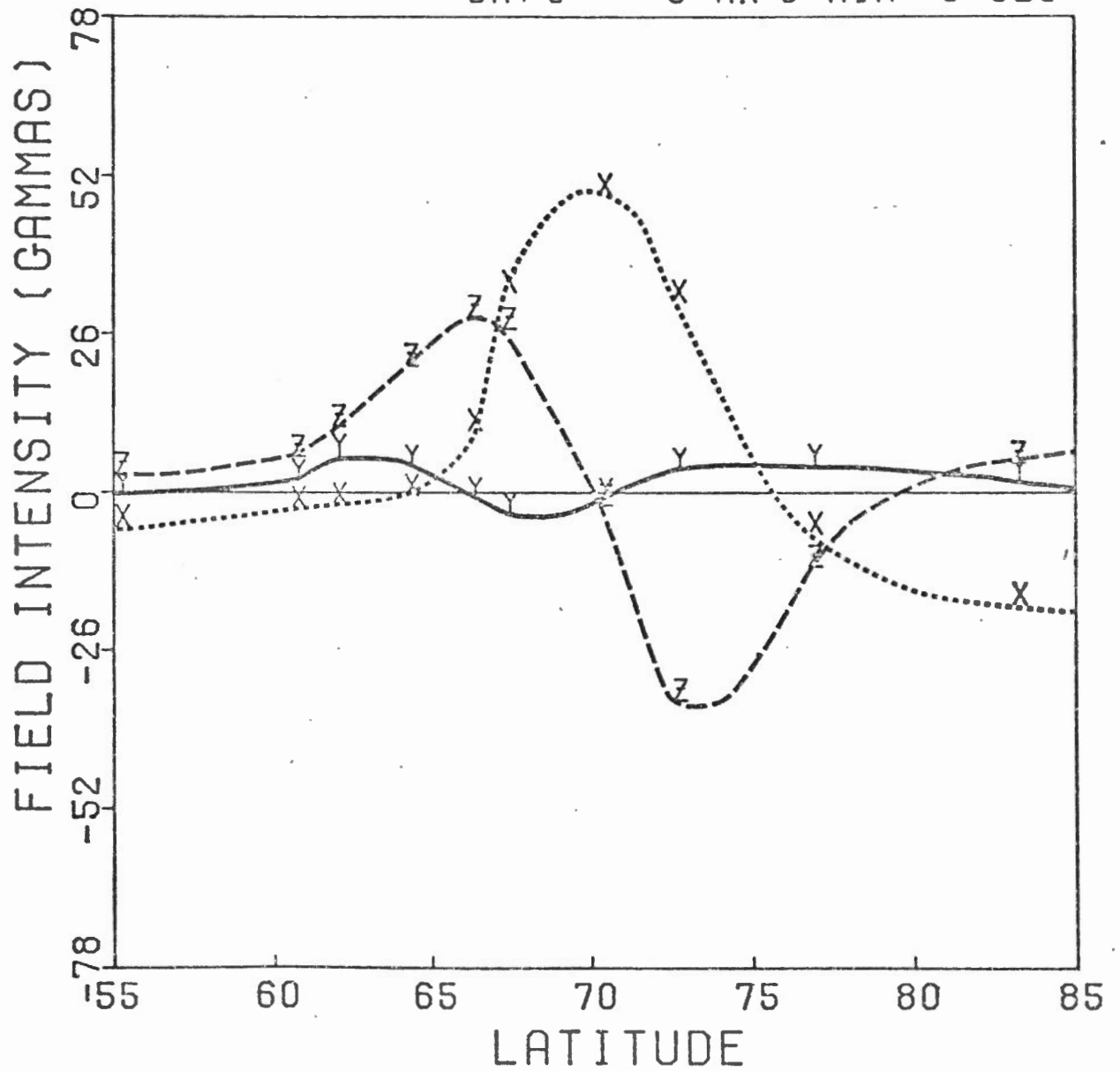


FIGURE 4(b). Same profile as in figure 4(a), but in a coordinate system in which the current flow is normal to the magnetometer line. In this example, the eastward current was flowing at an angle of  $29^\circ$  to the south.

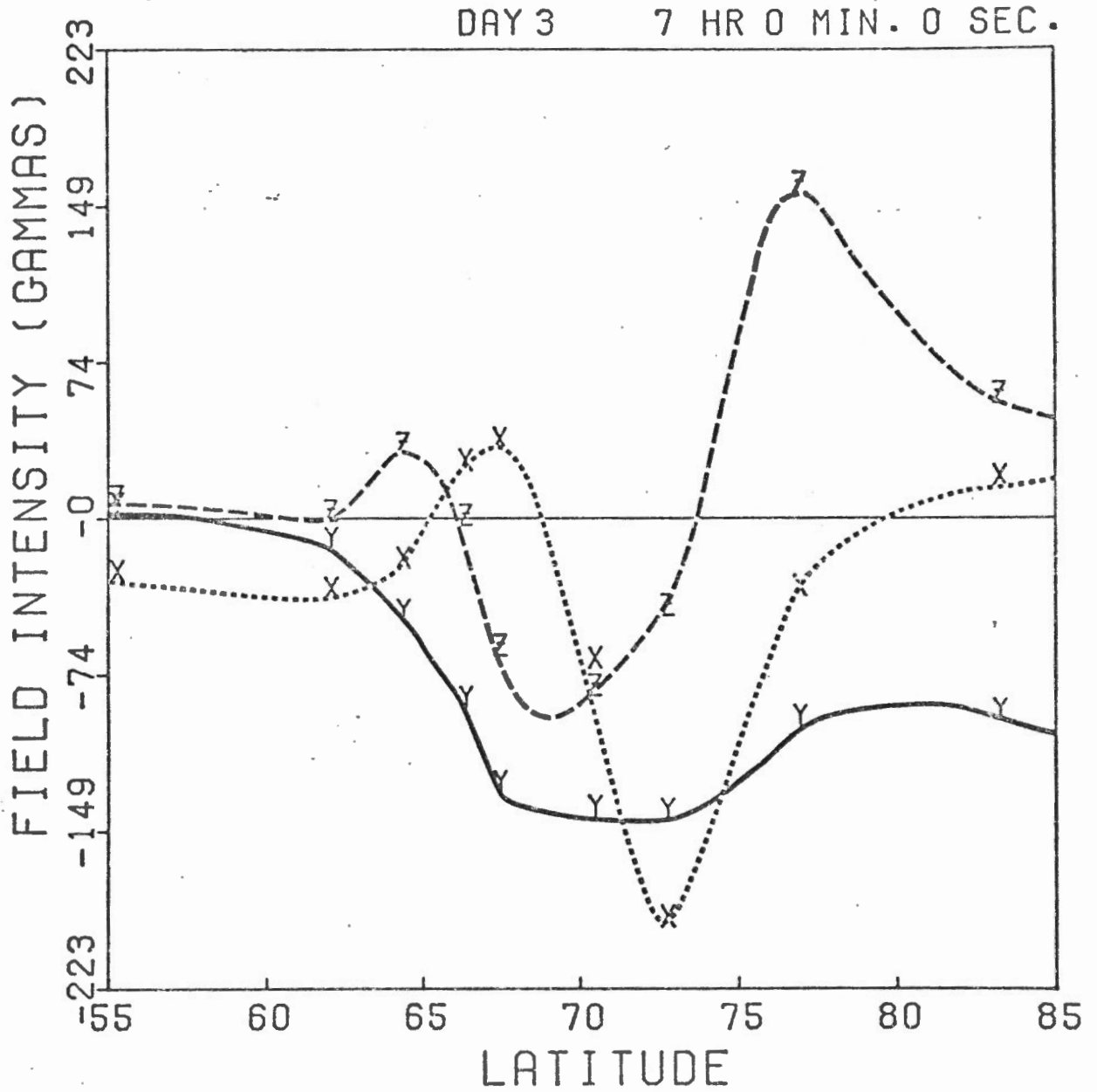


FIGURE 5.A latitude profile typical of the Harang Discontinuity.  
 Note that the east-west component (Y) is everywhere negative.

DAY 364 10HR 0 MIN. 0 SEC.

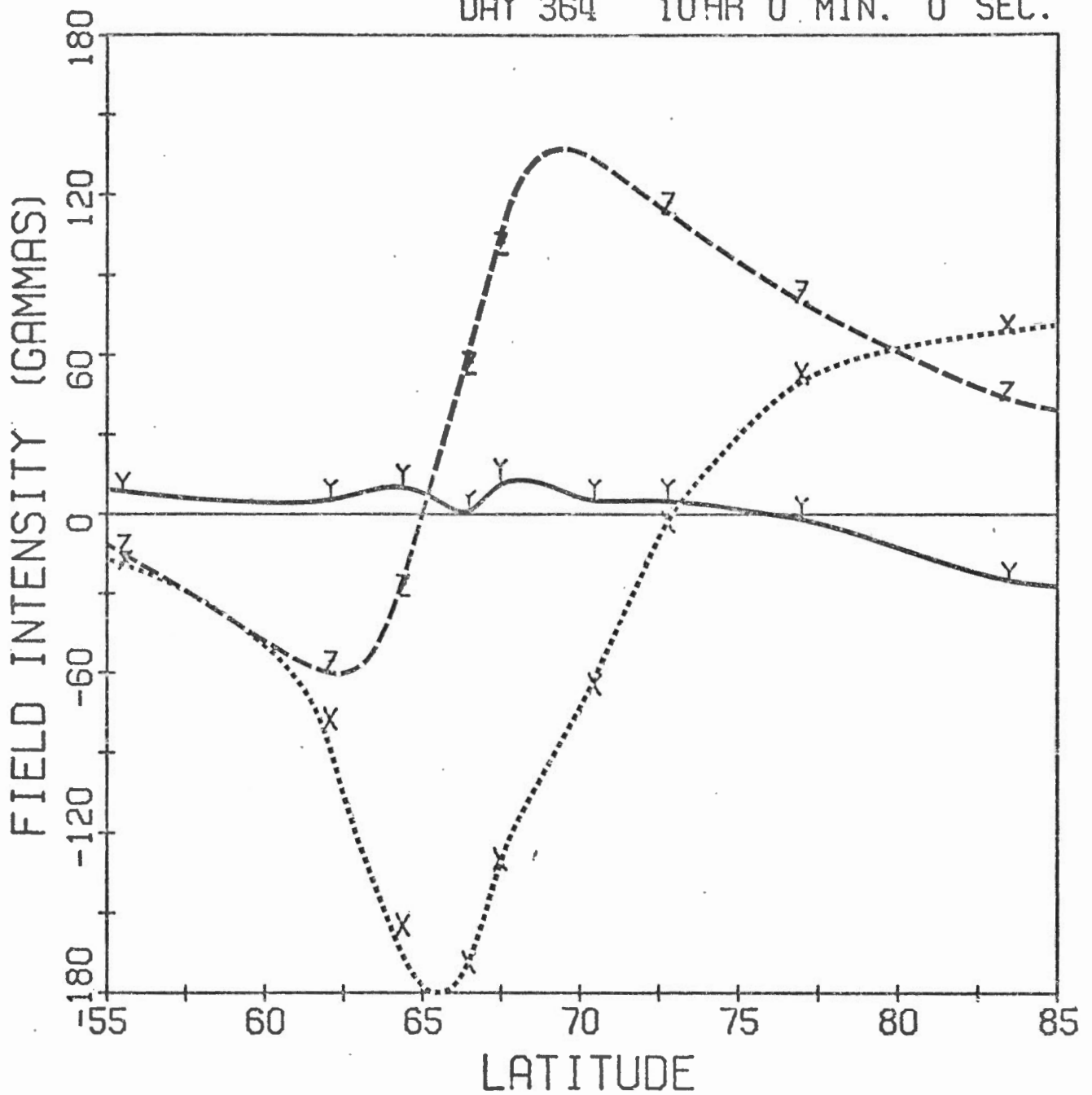


FIGURE 6(a). Latitude profile taken near the boundary between the westward electrojet region and the Harang Discontinuity.

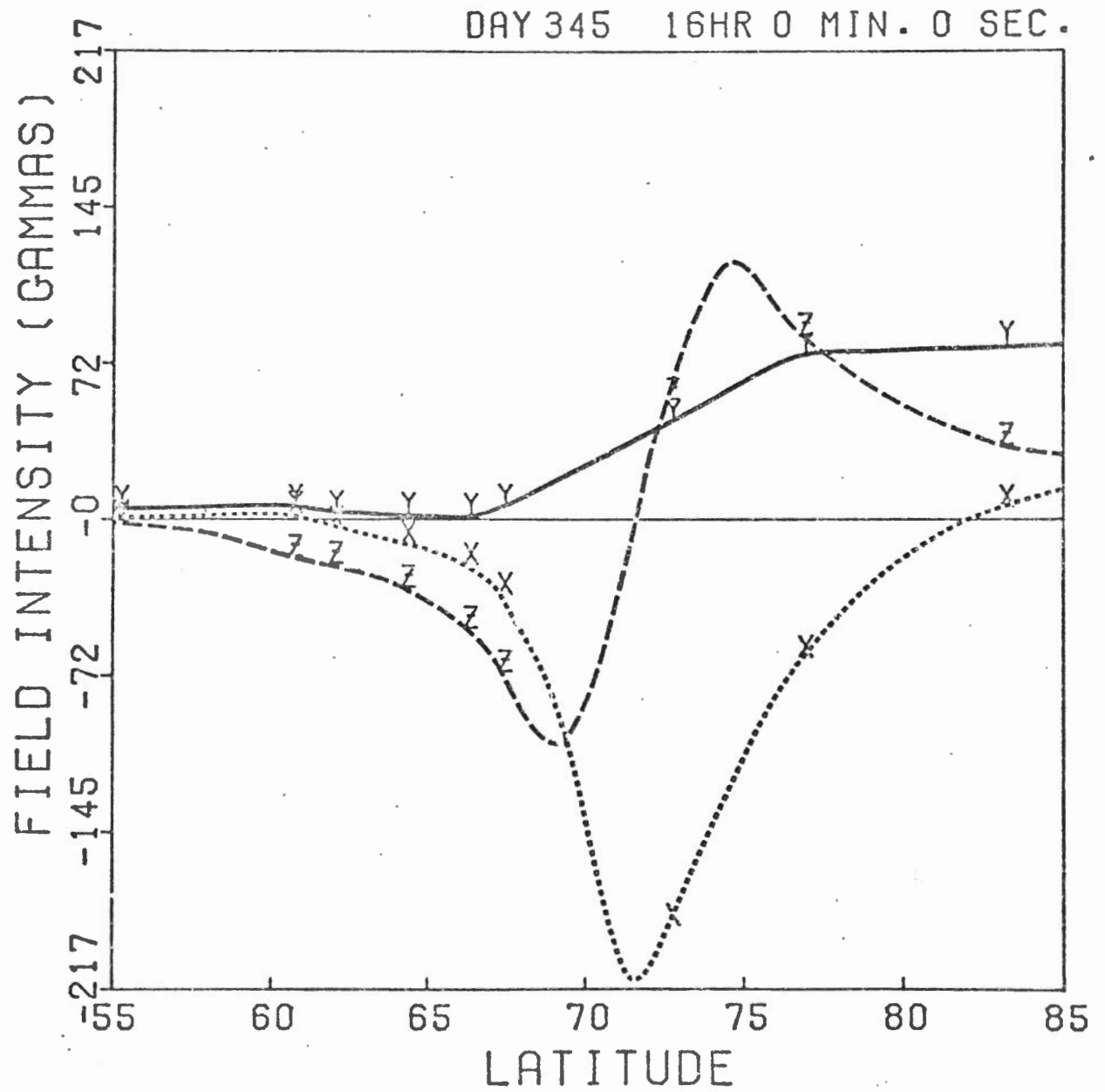


FIGURE 6(b). Latitude profile taken near local magnetic dawn.

DAY 338 20HR 0 MIN. 0 SEC.

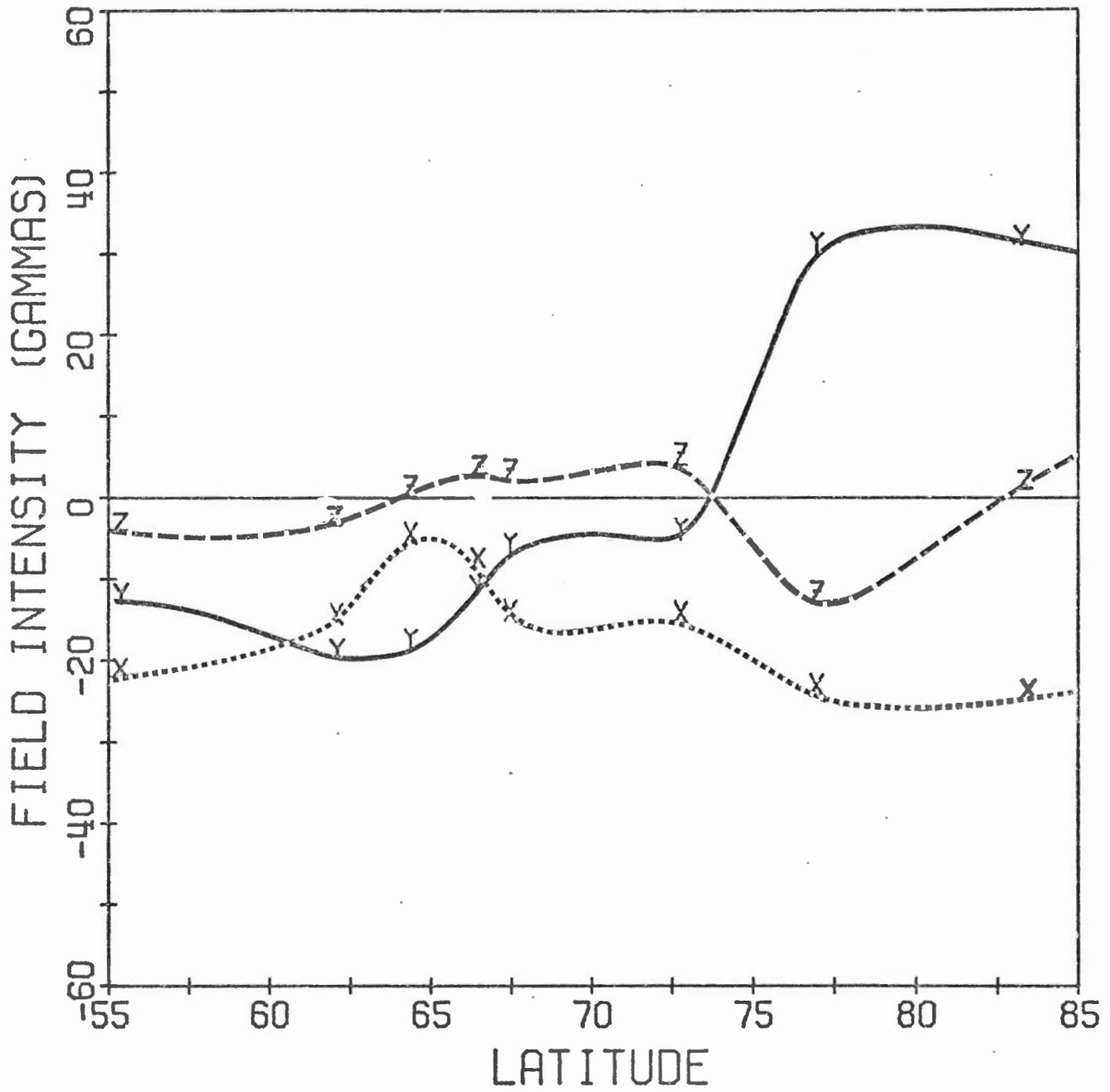


FIGURE 6(c). Latitude profile taken near local magnetic noon.

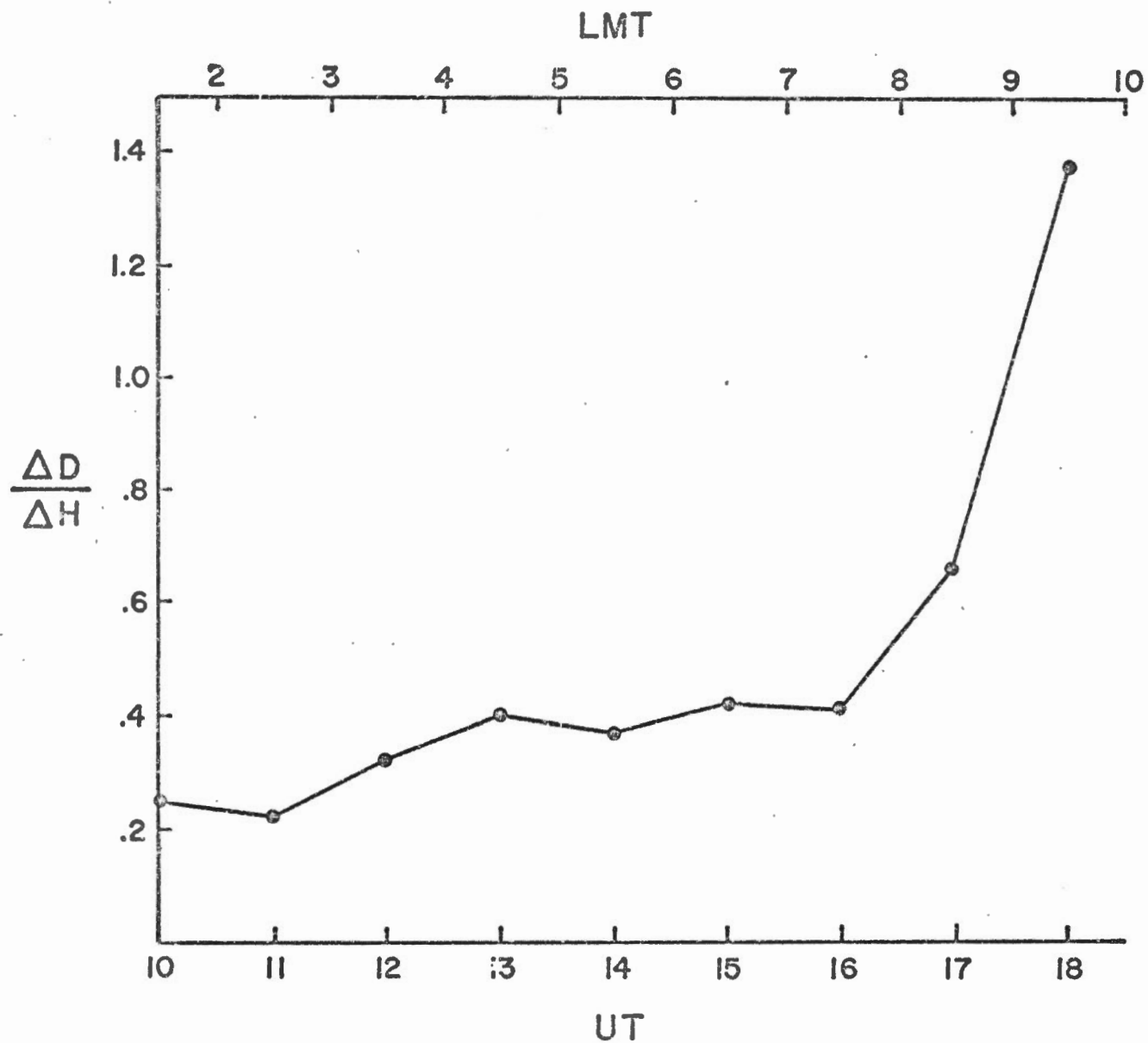


FIGURE 7. Ratio of the level shift in the east-west component ( $\Delta D$ ) to the peak north-south perturbation ( $\Delta H$ ) as a function of time.



DAY 332 18HR 0 MIN. 0 SEC.

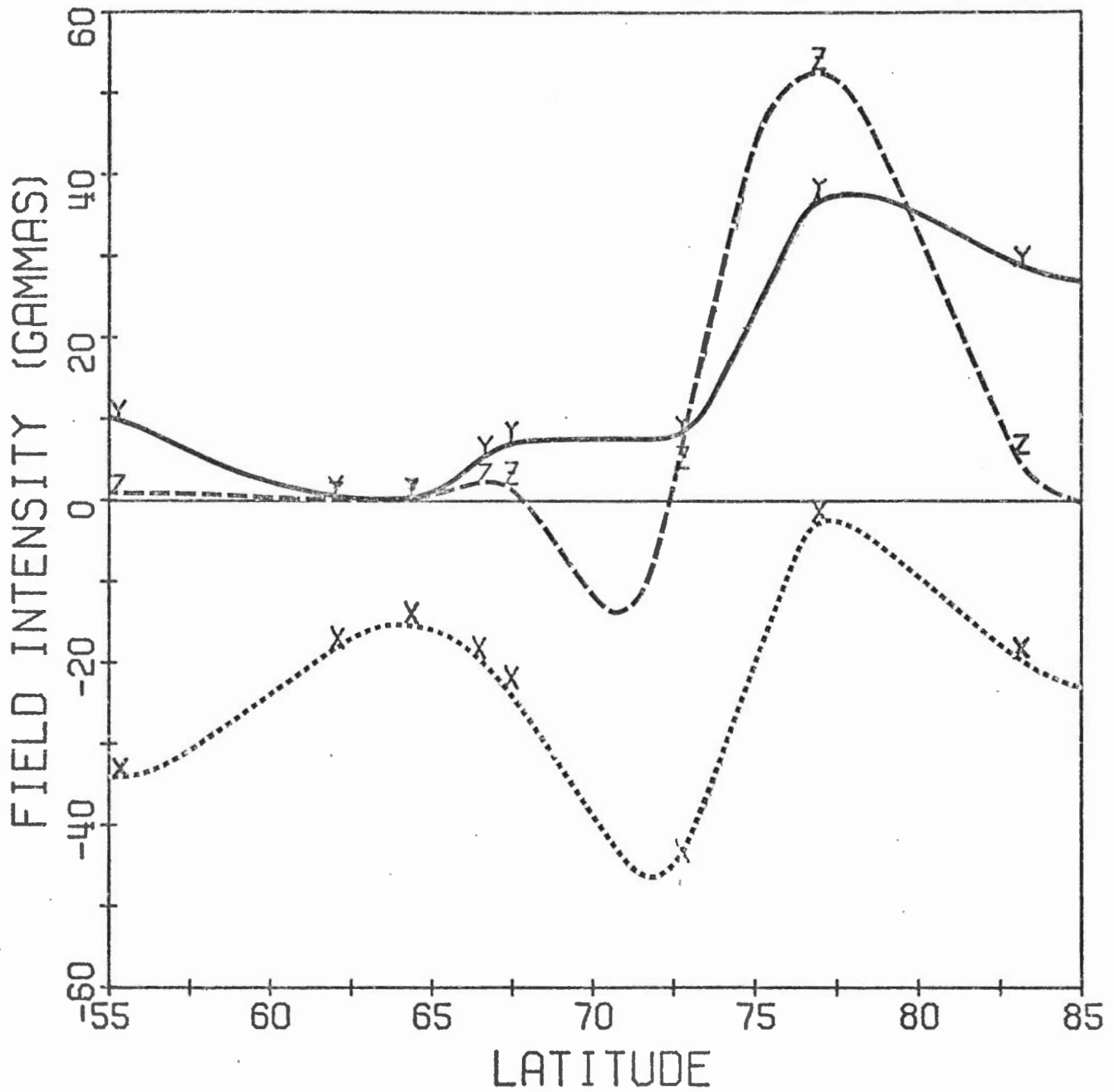


FIGURE 8(a). Latitude profile in the "zone of confusion" of Harang. Compare the character of the H(X) and D(Y) with those of figure 8(b).

DAY 332 19HR 0 MIN. 0 SEC

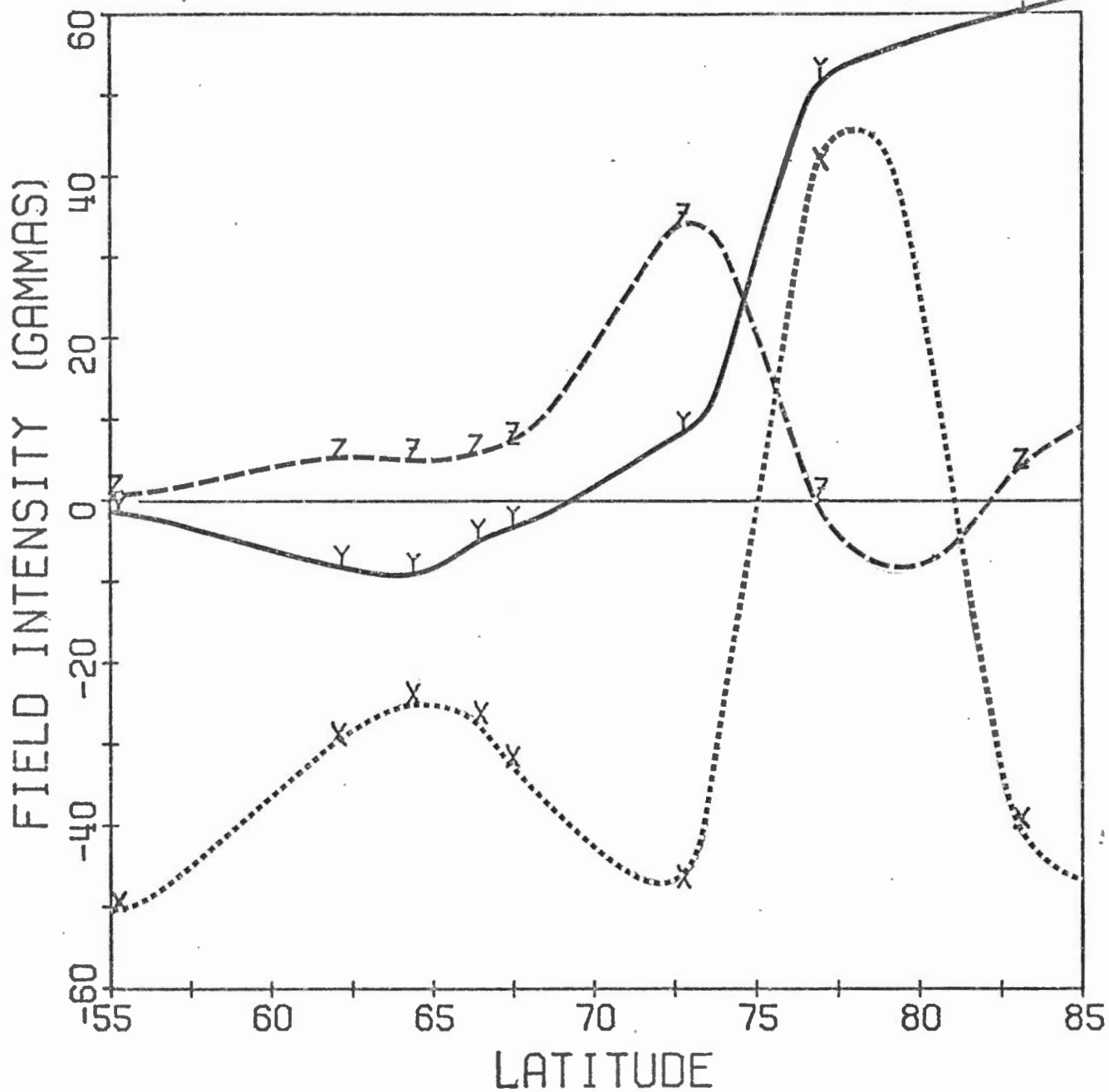


FIGURE 8(b). Latitude profile one hour later than figure 8(a).  
Note that the D(Y) component is similar to that of figure 8(a), but that the H(X) component has change markedly.

DAY 346 1 HR 0 MIN. 0 SEC.

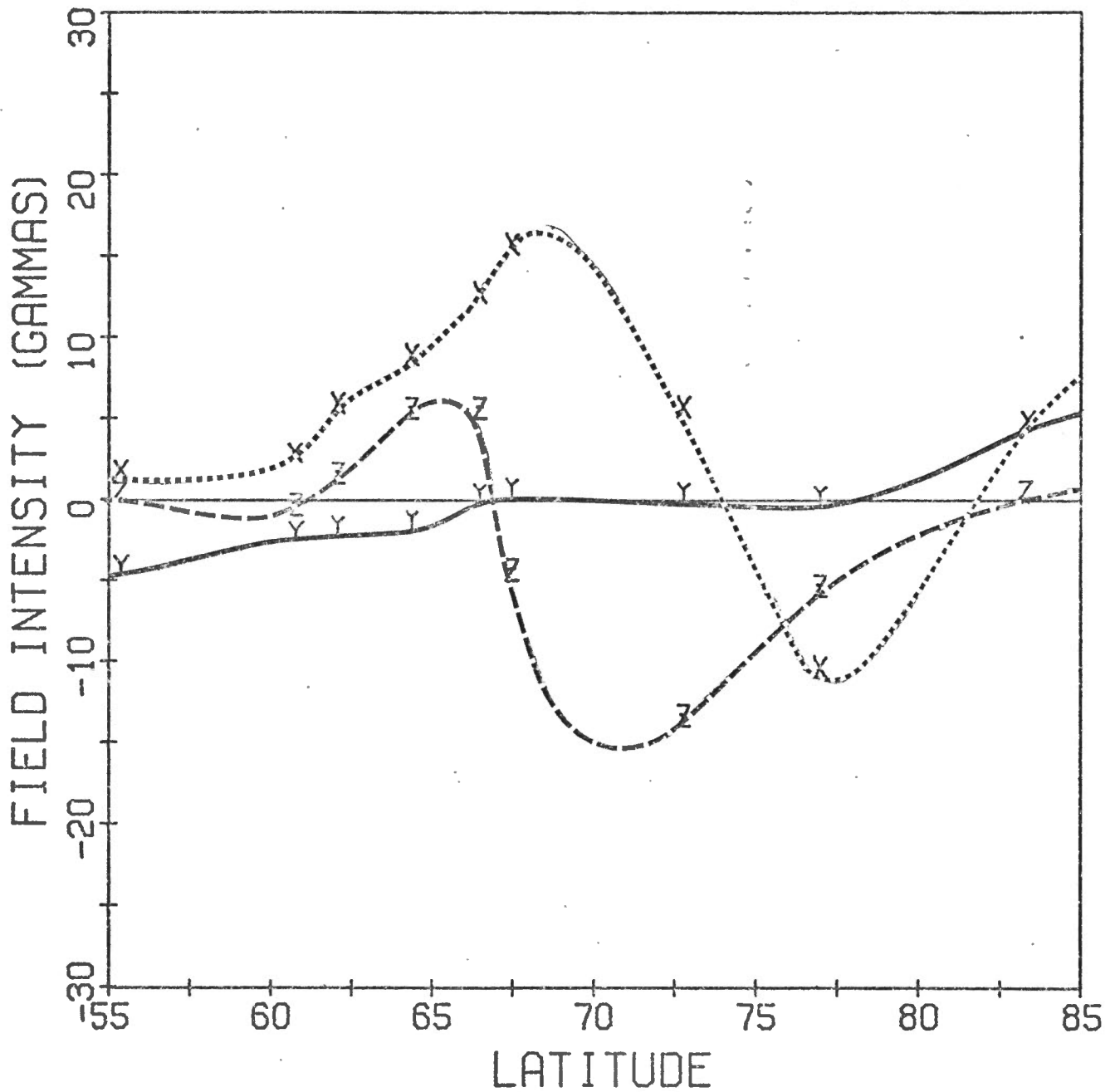


FIGURE 9. Latitude profile typical of those seen in the sector 1400 - 1900 LMT. Note the positive H(X) perturbation, indicating eastward electrojet, but the absence of a level shift in D(Y), indicating no net field aligned current.

DAY 346 5 HR 0 MIN. 0 SEC.

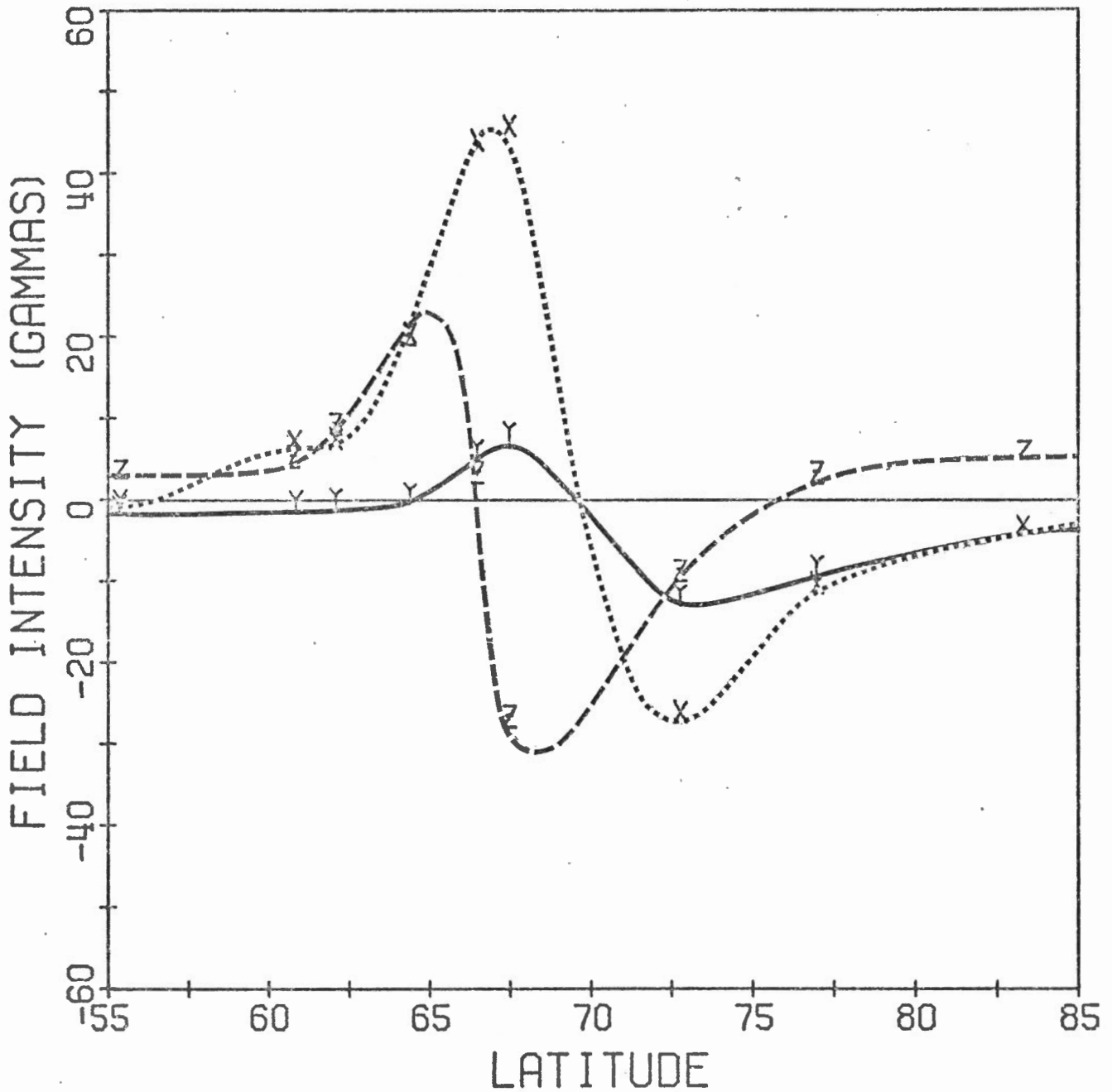


FIGURE 10. Latitude profile typical of those seen in the evening sector (1900-2200 LMT). Note the positive H(X) perturbation showing eastward electrojet, and the negative level shift in the D(Y) component, indicative of upward net field aligned current.

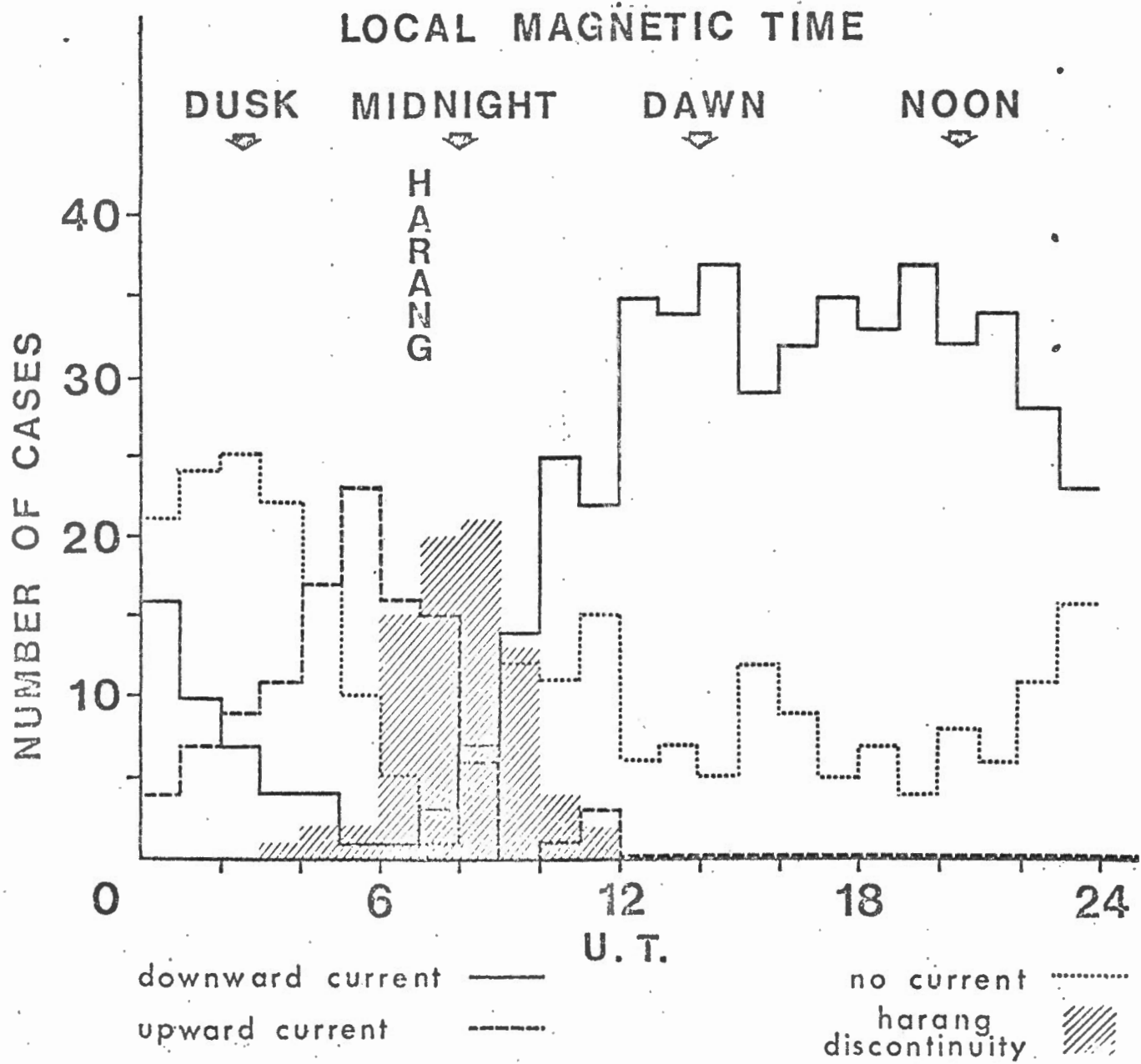


FIGURE 11. Histogram showing the distribution of net field aligned current as a function of UT. Approximate local magnetic times are shown across the top of the figure.

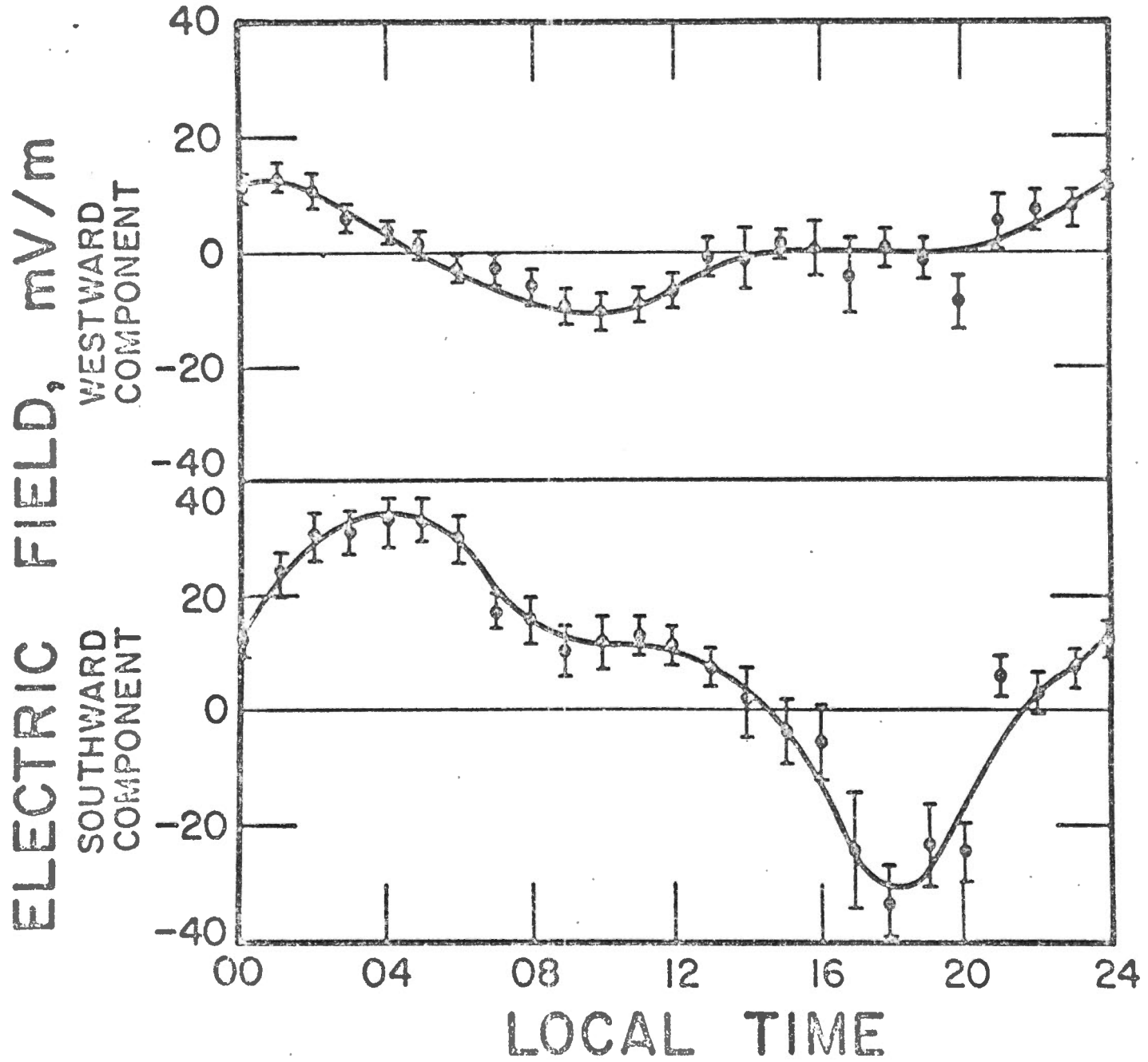


FIGURE 12. Diurnal variation in the ionospheric electric field in the region of the auroral oval. The time scale is local time. (0000 LT = 2230-2300 LMT). (From Mozer and Lucht. (1974))

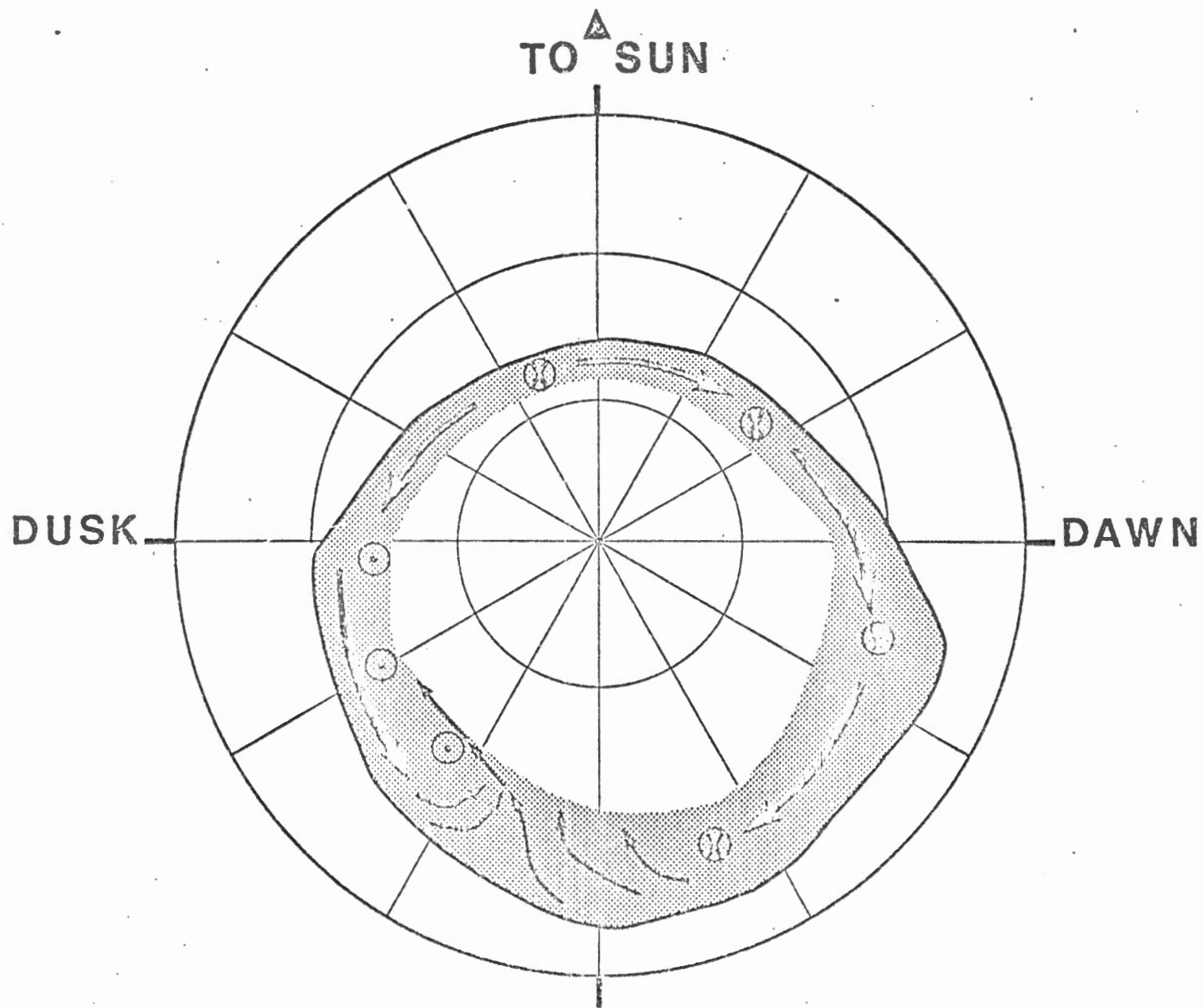


FIGURE 13. Model of the real current flow around the auroral oval. Net downward field aligned current feeds the westward electrojet from approximately noon to midnight. This current then diverges poleward and then westward and up the field lines, poleward of the evening eastward electrojet.